


## Three-body interaction near a narrow two-body zero crossing

A. Pricoupenko and D. S. Petrov 

*LPTMS, CNRS, Univ. Paris-Sud, Université Paris-Saclay, F-91405 Orsay, France*



(Received 4 July 2019; published 14 October 2019)

We calculate the effective three-body force for bosons interacting with each other by a two-body potential tuned to a narrow zero crossing in any dimension. We use the standard two-channel model parametrized by the background atom-atom interaction strength, the amplitude of the open-channel to closed-channel coupling, and the atom-dimer interaction strength. The three-body force originates from the atom-dimer interaction, but it can be dramatically enhanced for narrow crossings, i.e., for small atom-dimer conversion amplitudes. This effect can be used to stabilize quasi-two-dimensional dipolar atoms and molecules.

DOI: [10.1103/PhysRevA.100.042707](https://doi.org/10.1103/PhysRevA.100.042707)

### I. INTRODUCTION

In recent years, dilute weakly interacting bosons with intentionally weakened mean-field interactions have become one of the main attractions in the field of quantum gases. The weakness of the mean-field interaction in such systems makes higher-order terms relatively more important leading to dramatic effects. A prominent example is the observation of dilute quantum droplets in dipolar atoms [1–4] and in nondipolar mixtures [5–7]. Two-body interactions of different kinds (contact and dipole-dipole in the dipolar case and interspecies and intraspecies in the mixture case) are tuned to compete with each other such that the resulting weak overall attraction gets compensated by a higher-order Lee-Huang-Yang (LHY) term [8–10]. An impressive experimental progress has been made in the dipolar case on pursuing supersolidity through the formation of coherent arrays of quantum droplets [11–15].

All these achievements correspond to essentially three-dimensional setups well described by the Gross-Pitaevskii energy density functional with an additional local LHY term  $\propto n^{5/2}$ , where  $n$  is the density. However, there are various reasons to consider other configurations where the  $n^{5/2}$  term is absent or too weak (low-dimensional geometries, single-component contact-interacting atoms, etc.) In these cases, an effective three-body interaction, associated with a  $n^3$  term in the energy density, can become dominant if the leading-order two-body forces are suppressed. In particular, three-body forces have been considered in the context of droplet formation in three dimensions [16–19] and as a means for stabilizing supersolid phases of quasi-two-dimensional dipolar atoms or molecules [20]. Quite a few recent theory papers have discussed one-dimensional three-body-interacting systems, exploring the kinematic equivalence of the three-body scattering in one dimension and the two-body scattering in two dimensions (see, for example, Refs. [21–32]).

In this paper we analyze a simple mechanism for the emergence of an effective three-body interaction. Namely, we consider bosons interacting with each other by a potential tuned to a zero crossing near a narrow Feshbach resonance, where the conversion amplitude from atoms to closed-channel dimers is small and where the two-body scattering amplitude

is characterized by a large effective range  $R_e$ . The effective three-body force appears in this model when one takes into account the interaction between atoms and closed-channel dimers, characterized by the coupling strength  $g_{12}$ . We find that the three-body coupling constant  $g_3$  in  $D$  dimensions is proportional to  $R_e^D g_{12}$  and can thus be enhanced near narrow two-body zero crossings.

The paper is organized as follows. In Sec. II we introduce the two-channel model and perform its mean-field analysis. In the dilute limit the density of closed-channel dimers in the system scales as  $R_e^D n^2 \ll n$  and the effective three-body interaction emerges simply as the atom-dimer mean-field interaction energy  $\propto R_e^D g_{12} n^3$ . We show that this simple mechanism, applied to two-dimensional dipoles, generates conditions for observing supersolid phases predicted in Ref. [20].

In Secs. III and IV we turn to the few-body perspective and perform a detailed nonperturbative analysis of the two-body (Sec. III) and three-body (Sec. IV) problems with zero-range potentials. In particular, the three-body scattering length near a narrow two-body zero crossing is found for an arbitrary atom-dimer interaction strength in any dimension.

### II. MEAN-FIELD ANALYSIS

We start with the two-channel model described by the Hamiltonian [33]

$$\hat{H} = \int_{\mathbf{r}} \left\{ -\hat{\psi}_1^\dagger(\mathbf{r}) \frac{\nabla^2}{2} \hat{\psi}_1(\mathbf{r}) + \hat{\psi}_2^\dagger(\mathbf{r}) \left( -\frac{\nabla^2}{4} + v_0 \right) \hat{\psi}_2(\mathbf{r}) - \frac{\alpha}{2} [\hat{\psi}_1^\dagger(\mathbf{r}) \hat{\psi}_1^\dagger(\mathbf{r}) \hat{\psi}_2(\mathbf{r}) + \text{H.c.}] + \sum_{\sigma\sigma'} \frac{g_{\sigma\sigma'}}{2} \hat{n}_\sigma(\mathbf{r}) \hat{n}_{\sigma'}(\mathbf{r}) \right\}, \quad (1)$$

where  $\hat{\psi}_1$  and  $\hat{\psi}_2$  are, respectively, the annihilation operators of atoms and dimers,  $\hat{n}_\sigma$  are the corresponding density operators,  $v_0$  is the detuning parameter,  $g_{\sigma\sigma'}$  are interaction constants,  $\alpha$  is the atom-dimer conversion amplitude (without loss of generality assumed real and positive), and we have set  $\hbar$  and atom mass equal to 1. Hereafter,  $\int_{\mathbf{r}}$  denotes  $\int d^D r$ .

In the mean-field description of (1) we assume pure atomic and molecular condensates  $\hat{\psi}_\sigma = \sqrt{n_\sigma}$  with the same phase (which corresponds to the energy minimum for  $\alpha > 0$ ) [33]. We arrive at the energy density

$$E/L^D = v_0 n_2 - \alpha n_1 \sqrt{n_2} + \sum_{\sigma\sigma'} g_{\sigma\sigma'} n_\sigma n_{\sigma'}/2, \quad (2)$$

which we minimize with respect to  $n_2$  (or  $n_1$ ) keeping the total density  $n = n_1 + 2n_2$  constant. For positive  $v_0$  and small  $n$  the dimer population behaves quadratically in  $n$ ,

$$n_2 = \left( \frac{\alpha n}{2v_0} \right)^2 \left( 1 + \frac{4g_{11}v_0 - 2g_{12}v_0 - 3\alpha^2}{v_0^2} n \right) + O(n^4), \quad (3)$$

and the energy density reads

$$\frac{E}{L^D} = \left( \frac{g_{11}}{2} - \frac{\alpha^2}{4v_0} \right) \left( n^2 - \frac{\alpha^2}{v_0^2} n^3 \right) + \frac{g_{12}\alpha^2}{4v_0^2} n^3 + O(n^4). \quad (4)$$

The two-body zero crossing occurs at the detuning  $v_0 = \alpha^2/2g_{11}$ , where the first term in the right-hand side of Eq. (4) vanishes. One can then see that the residual three-body energy shift originates from the direct mean-field interaction of atoms with dimers. It equals  $g_{12}n_1n_2 \approx g_3n^3/3!$  with

$$g_3 = 6g_{12}g_{11}^2/\alpha^2 = 3g_{12}R_e^D. \quad (5)$$

The effective volume  $R_e^D = 2g_{11}^2/\alpha^2$  introduced in Eq. (5) characterizes the closed-channel population. Indeed, the density of dimers can be written as

$$n_2 \approx R_e^D n^2/2, \quad (6)$$

meaning that each pair of atoms is found in the closed-channel dimer state with probability  $(R_e/L)^D$ .

If  $g_{\sigma\sigma'}$  are of the same order of magnitude  $\sim g$ , the expansion (4) is in powers of  $R_e^D n$ , which we assume small. Then, at the zero crossing the three-body term gives the leading contribution to the energy density  $\sim gn^2(R_e^D n)^1$  and we neglect subleading terms such as, for instance, the dimer-dimer interaction  $\sim g_{22}\alpha^4 n^4/v_0^4 \sim gn^2(R_e^D n)^2$ . On the other hand, it may be interesting to keep a small but finite effective two-body interaction  $g_{\text{eff}} = g_{11} - \alpha^2/2v_0 \sim g(R_e^D n) \ll g$ , so that it can compete with the three-body term. It is also useful to note that the effective two-body interaction depends on the collisional momentum as  $g_{\text{eff}}(k) = g_{\text{eff}}(0) - R_e^D k^2$  (see [35] and Sec. III). However, if  $k \ll \sqrt{gn}$ , the corresponding effective-range correction gives a contribution to (4) much smaller than  $gn^2(R_e^D n)^1$ . We thus conclude that on this level of expansion we reduce (1) to the model of scalar bosons with local effective two-body and three-body interactions.

### A. Application to two-dimensional dipoles

Having in mind supersolid phases, which require a three-body repulsive force [20], let us perform the same mean-field analysis in the case of two-dimensional dipoles oriented perpendicular to the plane. Instead of pointlike interactions characterized by the momentum-independent constants  $g_{\sigma\sigma'}$  we now assume momentum-dependent pseudopotentials [20,34]

$$\tilde{V}_{\sigma\sigma'}(|\mathbf{k} - \mathbf{k}'|) = g_{\sigma\sigma'} - 2\pi d_\sigma d_{\sigma'} |\mathbf{k} - \mathbf{k}'|, \quad (7)$$

where  $\mathbf{k}$  and  $\mathbf{k}'$  are the incoming and outgoing relative momenta and  $d_1$  and  $d_2$  are dipole moments of atoms and dimers, respectively. The pseudopotential (7) is an effective potential valid only for the leading-order mean-field analysis at low momenta. Its coordinate representation

$$V_{\sigma\sigma'}(\mathbf{r} - \mathbf{r}') = \int \frac{d^2q}{(2\pi)^2} \tilde{V}_{\sigma\sigma'}(q) e^{i\mathbf{q}(\mathbf{r}-\mathbf{r}')} \quad (8)$$

has the long-distance asymptote  $d_\sigma d_{\sigma'}/r^3$  with the characteristic range  $r_{\sigma\sigma'}^* = 2\mu_{\sigma\sigma'} d_\sigma d_{\sigma'}$ , where  $\mu_{11} = 1/2$  and  $\mu_{12} = 2/3$  are the atom-atom and atom-dimer reduced masses, respectively.

Obviously, for homogeneous condensates the momentum-dependent part of (7) plays no role and our previous analysis holds. Namely, we arrive at the energy density  $E/L^2 = g_{\text{eff}} n^2/2 + g_3 n^3/6$ , where  $g_{\text{eff}} = g_{11} - \alpha^2/2v_0$  is tuned to be small and  $g_3$  is given by Eq. (5). Let us now assume that the atomic and dimer condensates are spatially modulated with a characteristic momentum  $k$  (in the supersolid phase the modulation is periodic). Then, the most important new terms in Eqs. (2) and (4) are the kinetic energy of the atomic component  $\sim nk^2$  and the momentum-dependent part of the atom-atom interaction  $\sim -r_{11}^* kn^2$ . Minimizing their sum with respect to  $k$  gives a contribution  $\epsilon_{\text{mod}} \sim -r_{11}^{*2} n^3$  to the energy density and the optimal modulation momentum  $k_{\text{min}} \sim r_{11}^* n$  [20]. One can check that other momentum-dependent terms are subleading. For instance, the kinetic energy of dimers  $\sim n_2 k^2$  and the momentum-dependent atom-dimer interaction  $\sim r_{12}^* knn_2$  carry an additional factor  $R_e^2 n \ll 1$ . It is important to mention that the density of dimers satisfies Eq. (6) locally, i.e.,  $n_2(\mathbf{r}) \approx R_e^D n^2(\mathbf{r})/2$ . Deviations from this relation, which follows from minimizing the first two terms in the right-hand side of Eq. (2), are energetically too costly. A change of  $n_2$  by, say, a factor of two compared to the optimal value would cost  $\sim g_{11} n^2 \gg gn^2(R_e^2 n)$  in the energy density.

This analysis leads us to the model of two-dimensional dipoles characterized by an effective two-body pseudopotential  $\tilde{V}(k) = g_{\text{eff}} - 2\pi d_1^2 k$  and local three-body term  $g_3 \delta(\mathbf{r}_1 - \mathbf{r}_2) \delta(\mathbf{r}_2 - \mathbf{r}_3)$ . The mean-field phase diagram of this model has been worked out in Ref. [20]. It has been shown that the stability of the system with respect to collapse is ensured by the repulsive three-body interaction term compensating the effectively attractive  $\epsilon_{\text{mod}}$ , which also scales as  $n^3$ . The supersolid stripe, honeycomb, and triangular phases are predicted when these two terms are comparable and  $g_{\text{eff}} < 0$ . To give a concrete example, the four-critical point where the three supersolid phases meet with one another and with the uniform phase (this is also the point where the roton minimum touches zero) is characterized by  $g_{12}R_e^2 = 2(\pi r_{11}^*)^2$  and  $nR_e^2 = |g_{\text{eff}}|/g_{12}$ .

### B. Inelastic losses

Collisions of atoms with closed-channel dimers can lead to the relaxation to more deeply bound molecular states. The rate of this process in a unit volume is given by  $\alpha_r n_1 n_2$ , where  $\alpha_r$  is the relaxation rate constant. In our model this corresponds to the atom loss rate  $\dot{n} = -(3/2)\alpha_r R_e^D n^3$ , and we see that this effective three-body loss gets enhanced with increasing  $R_e$  in the same manner as the elastic three-body

interaction (5). In fact, the atom-dimer relaxation can be mathematically modeled by allowing  $g_{12}$  to be complex. Shotan and co-workers [35] have measured the three-body loss rate constant near a two-body zero crossing in three dimensions. They argue that this quantity is proportional to  $R_e^4$ . Here we claim a slightly different scaling ( $\propto R_e^3$ ), valid when  $R_e$  is much larger than the van der Waals range.

For Feshbach molecules of the size of the van der Waals length  $\alpha_r$  is typically of the same order of magnitude as  $g_{12}$ . The lifetime of the sample is thus comparable to the time scale associated with the elastic three-body energy shift. There are, however, ways of overcoming this problem. For dipoles oriented perpendicular to the plane in the quasi-two-dimensional geometry inelastic processes are suppressed by the predominantly repulsive dipolar tail. For instance, for Dy the atom-dimer dipolar length  $r_{12}^*$  can reach about 50 nm depending on the magnetic moment of the closed-channel dimer. The confinement of frequency  $\omega = 2\pi \times 100$  kHz for this system gives the oscillator length  $\sqrt{\hbar/2\mu_{12}\omega} \approx 21$  nm. Under these conditions one expects a noticeable reduction of the relaxation rate [36–38]. This mechanism may work also for dipolar molecules where larger values of  $r_{12}^*$  can be reached.

A different approach to this problem is to consider closed-channel dimers which are weakly bound and have a halo character, i.e., well extended beyond the support of the potential. A specific way of generating three-body interactions in this manner has been proposed by one of us in Ref. [17]; two atoms in state 1 collide and both go to another internal state 1' where they form an extended molecular state. The effective three-body force is then due to a repulsive mean-field interaction between atoms 1' and a third atom in state 1. In this case, the relaxation is slow since the dimer is not “preformed.”

### III. REGULARIZED MODEL AND TWO-BODY PROBLEM

We now go back to the model (1), try to analyze it from the few-body viewpoint, and characterize the three-body interaction beyond the mean-field result (5) (also trying to determine its validity regime). Clearly, at some point the strength of the background atom-atom interaction becomes a relevant parameter (not just the ratio  $g_{11}/\alpha$ ). One also observes that the pointlike interaction and conversion terms in Eq. (1) lead to divergences and have to be regularized in dimensions  $D > 1$ , which necessitates an additional parameter (a short-range or high-momentum cutoff).

In order to regularize the model (1) we use the delta-shell pseudopotential representation [39,40] with a finite range  $r_0$ . Namely, we rewrite Eq. (1) as

$$\begin{aligned} \hat{H} = & \int_{\mathbf{r}} -\hat{\psi}_1^\dagger(\mathbf{r}) \frac{\nabla^2}{2} \hat{\psi}_1(\mathbf{r}) + \hat{\psi}_2^\dagger(\mathbf{r}) \left( -\frac{\nabla^2}{4} + \nu_0 \right) \hat{\psi}_2(\mathbf{r}) \\ & + \sum_{\sigma\sigma'} \frac{g_{\sigma\sigma'}}{2} \int_{\mathbf{r}} \int_{\mathbf{y}} \tilde{\delta}_{r_0}(\mathbf{y}) \hat{n}_\sigma(\mathbf{r} + \mathbf{y}/2) \hat{n}_{\sigma'}(\mathbf{r} - \mathbf{y}/2) \\ & - \frac{\alpha}{2} \int_{\mathbf{r}} \int_{\mathbf{y}} \tilde{\delta}_{r_0}(\mathbf{y}) [\hat{\psi}_1^\dagger(\mathbf{r} + \mathbf{y}/2) \hat{\psi}_1^\dagger(\mathbf{r} - \mathbf{y}/2) \hat{\psi}_2(\mathbf{r}) + \text{H.c.}], \end{aligned} \quad (9)$$

where  $\tilde{\delta}_{r_0}(\mathbf{y}) = \delta(|\mathbf{y}| - r_0)/S_D(r_0)$  is the normalized delta shell with  $S_1(r_0) = 2$ ,  $S_2(r_0) = 2\pi r_0$ , and  $S_3(r_0) = 4\pi r_0^2$ . The range  $r_0$  should be understood as the smallest length scale in our problem. It does not enter in the final formulas and it is just a convenient way to regularize the problem without using zero-range pseudopotentials, which have different forms in different dimensions. In the one-dimensional case  $r_0$  can be set to zero from the very beginning, but we keep it finite in order to use the same formalism for the cases with different  $D$ . Note also that we do not intend to consider effects of scattering with angular momenta  $l \neq 0$ . This is to say that, as  $r_0$  is decreased, the coupling constants  $g_{\sigma\sigma'}$  and  $\alpha$  are tuned to reproduce desired (physical)  $R_e$  and  $a_{\sigma\sigma'}$  only for the  $s$ -wave channel. Then, in the limit  $r_0 \rightarrow 0$ , the terms  $g_{\sigma\sigma'} \tilde{\delta}_{r_0}(\mathbf{y})$  and  $\alpha \tilde{\delta}_{r_0}(\mathbf{y})$  are too weak to induce any scattering for  $l > 0$ .

A stationary two-body state with zero center-of-mass momentum and  $l = 0$  in the two-channel models (1) or (9) is represented by

$$\int_{\mathbf{c}} \int_{\mathbf{y}} \Psi(\mathbf{y}) \hat{\psi}_1^\dagger(\mathbf{c} + \mathbf{y}/2) \hat{\psi}_1^\dagger(\mathbf{c} - \mathbf{y}/2) |0\rangle + \int_{\mathbf{c}} \phi \hat{\psi}_2^\dagger(\mathbf{c}) |0\rangle, \quad (10)$$

where  $|0\rangle$  is the vacuum state. Acting on (10) by the operator  $\hat{H} - E$ , and requiring that the result vanish, we get the coupled Schrödinger equations at energy  $E$ ,

$$[-\nabla_{\mathbf{y}}^2 - E + g_{11} \tilde{\delta}_{r_0}(\mathbf{y})] \Psi(\mathbf{y}) = \alpha \tilde{\delta}_{r_0}(\mathbf{y}) \phi/2, \quad (11)$$

$$(\nu_0 - E) \phi = \alpha \Psi(r_0), \quad (12)$$

which, upon eliminating the closed-channel amplitude  $\phi$ , become

$$[-\nabla_{\mathbf{y}}^2 - E + g_{\text{eff}}(E) \tilde{\delta}_{r_0}(\mathbf{y})] \Psi(\mathbf{y}) = 0, \quad (13)$$

with

$$g_{\text{eff}}(E) = g_{11} + \frac{1}{2} \frac{\alpha^2}{E - \nu_0}. \quad (14)$$

The zero crossing condition at zero energy thus reads

$$\nu_0 = \alpha^2/2g_{11}. \quad (15)$$

We also introduce the effective range by the formula

$$R_e^D = \alpha^2/2\nu_0^2 > 0, \quad (16)$$

which characterizes the small- $E$  asymptote  $g_{\text{eff}}(E) = g_{\text{eff}}(0) - R_e^D E + O(E^2)$  (cf. [35]). At the crossing Eq. (16) is consistent with our earlier definition of  $R_e$  introduced in Eq. (5). As we have mentioned,  $R_e^D$  is also related to the closed-channel occupation. Indeed, from the normalization integral of Eq. (10) one finds that the closed-channel to open-channel probability ratio equals  $|\phi|^2 / \int_{\mathbf{y}} 2|\Psi(\mathbf{y})|^2 = |\phi|^2 / [2L^D |\Psi(r_0)|^2]$ , where we have used the fact that at the crossing  $\Psi(\mathbf{y}) = \Psi(r_0)$ . On the other hand, from Eq. (12) one obtains  $|\phi|^2 = 2R_e^D |\Psi(r_0)|^2$  for  $|E| \ll |\nu_0|$ , which gives the result claimed in Sec. II. Namely, the probability for two atoms to be in the closed-channel dimer state equals  $(R_e/L)^D$ .

Eventually, we will need to express our results in terms of the scattering lengths  $a_{\sigma\sigma'}$  and the effective range  $R_e$  rather than in terms of the bare  $r_0$ -dependent quantities  $g_{\sigma\sigma'}$ ,  $\alpha$ , and

$v_0$ . Relations between  $g_{\sigma\sigma'}$  and  $a_{\sigma\sigma'}$  are obtained by solving the scattering problem at zero collision energy and by looking at the long-distance asymptote of the two-body wave function. Namely, the zero-energy Schrödinger equation reads

$$[-\nabla_{\mathbf{y}}^2 + 2\mu_{\sigma\sigma'}g_{\sigma\sigma'}\tilde{\delta}_{r_0}(\mathbf{y})]\Psi(\mathbf{y}) = 0. \quad (17)$$

In one dimension the (unnormalized) solution is

$$\Psi(\mathbf{y}) = \begin{cases} 1, & |\mathbf{y}| < r_0, \\ 1 + \mu_{\sigma\sigma'}g_{\sigma\sigma'}(|\mathbf{y}| - r_0), & |\mathbf{y}| > r_0, \end{cases} \quad (18)$$

from which we see that

$$a_{\sigma\sigma'} = r_0 - 1/\mu_{\sigma\sigma'}g_{\sigma\sigma'}. \quad (19)$$

In the limit  $r_0 \rightarrow 0$  we recover the usual relation  $g_{\sigma\sigma'} = -1/\mu_{\sigma\sigma'}a_{\sigma\sigma'}$ . In two dimensions the solution of Eq. (17) reads

$$\Psi(\mathbf{y}) = \begin{cases} 1, & |\mathbf{y}| < r_0, \\ 1 + \mu_{\sigma\sigma'}g_{\sigma\sigma'} \ln(|\mathbf{y}|/r_0)/\pi, & |\mathbf{y}| > r_0 \end{cases} \quad (20)$$

and one has

$$\mu_{\sigma\sigma'}g_{\sigma\sigma'} = \pi / \ln(r_0/a_{\sigma\sigma'}). \quad (21)$$

In three dimensions

$$\Psi(\mathbf{y}) = \begin{cases} 1, & |\mathbf{y}| < r_0, \\ 1 - \mu_{\sigma\sigma'}g_{\sigma\sigma'}/2\pi|\mathbf{y}| + \mu_{\sigma\sigma'}g_{\sigma\sigma'}/2\pi r_0, & |\mathbf{y}| > r_0, \end{cases} \quad (22)$$

from which we obtain

$$1/a_{\sigma\sigma'} = 2\pi/\mu_{\sigma\sigma'}g_{\sigma\sigma'} + 1/r_0. \quad (23)$$

We now analyze conditions for having two-body bound states at the two-body zero crossing, in particular, having in mind the three-body recombination to these states when considering the three-body problem. We just note that solutions of Eq. (13) at distances  $|\mathbf{y}| \ll 1/\sqrt{|E|}$  in different dimensions are given, respectively, by Eqs. (18), (20), and (22) with  $\sigma = \sigma' = 1$  and with  $g_{11}$  substituted by  $g_{\text{eff}}(E)$ . We then match these asymptotes with the decaying solutions  $\Psi^{(D=1)}(\mathbf{y}) \propto \exp(\kappa|\mathbf{y}|)$ ,  $\Psi^{(D=2)}(\mathbf{y}) \propto K_0(\kappa|\mathbf{y}|)$ , and  $\Psi^{(D=3)}(\mathbf{y}) \propto \exp(-\kappa|\mathbf{y}|)/|\mathbf{y}|$ , where  $\kappa = \sqrt{-E}$ . This matching procedure gives the following equations for the determination of  $\kappa$  ( $\gamma \approx 0.577$  is the Euler constant):

$$(\kappa R_e)^2(a_{11}/R_e) - \kappa R_e = 2, \quad D = 1, \quad (24)$$

$$(\kappa R_e)^2 \ln(\kappa a_{11} e^\gamma / 2) = 2\pi, \quad D = 2, \quad (25)$$

$$(\kappa R_e)^3 - (\kappa R_e)^2(R_e/a_{11}) = 4\pi, \quad D = 3. \quad (26)$$

Analyzing these equations we find that in one dimension there is no two-body bound state, if  $a_{11} < 0$  (or  $g_{11} > 0$ ). In higher dimensions we always have a bound state, but it becomes deep in the limit of small positive  $a_{11}$  ( $E \propto -1/a_{11}^2$ ). In principle, the case of a weak repulsive background atom-atom interaction can also be realized by a finite-range repulsive potential (in the mean-field spirit of Sec. II). Then, the dimer states given by Eqs. (24)–(26) are spurious, consistent with the fact that the zero-range theory can no longer be used at such high momenta.

#### IV. THREE-BODY PROBLEM

Similar to Eq. (10) a stationary state of three atoms with zero center-of-mass momentum can be written in the form

$$\begin{aligned} & \int_{\mathbf{c}} \int_{\mathbf{x}} \int_{\mathbf{y}} \Psi(\mathbf{x}, \mathbf{y}) \hat{\psi}_1^\dagger(\mathbf{c} - \mathbf{x}/2\sqrt{3} - \mathbf{y}/2) \hat{\psi}_1^\dagger(\mathbf{c} - \mathbf{x}/2\sqrt{3} + \mathbf{y}/2) \\ & \times \hat{\psi}_1^\dagger(\mathbf{c} + \mathbf{x}/\sqrt{3}) |0\rangle + \int_{\mathbf{c}} \int_{\mathbf{x}} \phi(\mathbf{x}) \hat{\psi}_2^\dagger(\mathbf{c} - \mathbf{x}/2\sqrt{3}) \\ & \times \hat{\psi}_1^\dagger(\mathbf{c} + \mathbf{x}/\sqrt{3}) |0\rangle, \end{aligned} \quad (27)$$

where  $\mathbf{c}$  is the center-of-mass coordinate and the relative Jacobi coordinates are

$$\begin{aligned} \mathbf{x} &= (2\mathbf{r}_1 - \mathbf{r}_2 - \mathbf{r}_3)/\sqrt{3}, \\ \mathbf{y} &= \mathbf{r}_3 - \mathbf{r}_2. \end{aligned} \quad (28)$$

Let us introduce operators  $\hat{P}_+$  and  $\hat{P}_-$  which exchange the first atom with the second and the third, respectively. Acting by these operators on an arbitrary function  $F(\mathbf{x}, \mathbf{y})$  results in

$$\hat{P}_\pm F(\mathbf{x}, \mathbf{y}) = F(-\mathbf{x}/2 \mp \sqrt{3}\mathbf{y}/2, -\sqrt{3}\mathbf{x}/2 \pm \mathbf{y}/2). \quad (29)$$

The open-channel wave function  $\Psi(\mathbf{x}, \mathbf{y})$  is invariant with respect to these permutations.

The coupled Schrödinger equations for  $\Psi$  and  $\phi$  read

$$\begin{aligned} & [-\nabla_{\mathbf{x}}^2 - \nabla_{\mathbf{y}}^2 - E + g_{11}(1 + \hat{P}_+ + \hat{P}_-)\tilde{\delta}_{r_0}(\mathbf{y})]\Psi(\mathbf{x}, \mathbf{y}) \\ & = \alpha(1 + \hat{P}_+ + \hat{P}_-)\tilde{\delta}_{r_0}(\mathbf{y})\phi(\mathbf{x})/2, \end{aligned} \quad (30)$$

$$[-\nabla_{\mathbf{x}}^2 - v_0 - E + g_{12}\tilde{\delta}_{r_0}(\sqrt{3}\mathbf{x}/2)]\phi(\mathbf{x}) = \alpha\Psi(\mathbf{x}, r_0), \quad (31)$$

where  $\Psi(\mathbf{x}, r_0)$  in the right-hand side of Eq. (31) denotes the projection on the  $s$ -wave channel in the coordinate  $\mathbf{y}$ , i.e., the angular average  $\langle \Psi(\mathbf{x}, r_0\hat{\mathbf{y}}) \rangle_{\hat{\mathbf{y}}}$ . The difference between  $\Psi(\mathbf{x}, r_0\hat{\mathbf{y}})$  and  $\Psi(\mathbf{x}, r_0)$ , which accounts for non- $s$ -wave scattering channels, vanishes in the limit  $r_0 \rightarrow 0$  and we will thus make the replacement  $\tilde{\delta}_{r_0}(\mathbf{y})\Psi(\mathbf{x}, \mathbf{y}) \rightarrow \tilde{\delta}_{r_0}(\mathbf{y})\Psi(\mathbf{x}, r_0)$  in Eq. (30). Then, it is convenient (the reason will become clear below) to introduce an auxiliary function  $f(\mathbf{x})$  such that

$$\Psi(\mathbf{x}, r_0) = -f(\mathbf{x})/g_{11} + \alpha\phi(\mathbf{x})/2g_{11}. \quad (32)$$

We now eliminate  $\Psi$  from Eqs. (30) and (31) in favor of  $f$  and thus derive coupled equations for  $f$  and  $\phi$ . To this end we note that with the use of (32) Eq. (30) becomes

$$(-\nabla_{\mathbf{x}}^2 - \nabla_{\mathbf{y}}^2 - E)\Psi(\mathbf{x}, \mathbf{y}) = (1 + \hat{P}_+ + \hat{P}_-)\tilde{\delta}_{r_0}(\mathbf{y})f(\mathbf{x}). \quad (33)$$

Equation (33) can now be solved with respect to  $\Psi$  by using the Green function  $G_E^{(2D)}$  of the  $2D$ -dimensional Helmholtz operator in the left-hand side (see, for example, Ref. [41]). This procedure gives

$$\begin{aligned} \Psi(\mathbf{x}, r_0) &= \Psi_0(\mathbf{x}, 0) + \int_{\mathbf{x}'} \left\{ G_E^{(2D)} \left[ \sqrt{(\mathbf{x} - \mathbf{x}')^2 + r_0^2} \right] \right. \\ & \left. + \sum_{\pm} G_E^{(2D)}(\sqrt{x^2 \pm \mathbf{x}\mathbf{x}' + x'^2}) \right\} f(\mathbf{x}'), \end{aligned} \quad (34)$$

where  $\Psi_0(\mathbf{x}, \mathbf{y})$  is any solution of  $(-\nabla_{\mathbf{x}}^2 - \nabla_{\mathbf{y}}^2 - E)\Psi_0(\mathbf{x}, \mathbf{y}) = 0$ . In Eq. (34) we have already taken the limit  $r_0 \rightarrow 0$ , where it exists. With the use of Eq. (34) the function



$\Psi(\mathbf{x}, r_0)$  can now be eliminated from Eqs. (32) and (31). Here we explicitly write down the resulting coupled equations for  $f$  and  $\phi$  at the two-body zero crossing ( $v_0 = \alpha^2/2g_{11}$ ) and at zero energy ( $E = 0, \Psi_0 = 1$ ):

$$\hat{L}f(\mathbf{x}) + f(\mathbf{x})/g_{11} = \phi(\mathbf{x})/\sqrt{2R_e^D} - 1, \quad (35)$$

$$[-\nabla_{\mathbf{x}}^2 + g_{12}\delta_{r_0}(\sqrt{3}x/2)]\phi(\mathbf{x}) = -\sqrt{2/R_e^D}f(\mathbf{x}), \quad (36)$$

where  $\hat{L}$  is the integral operator in the right-hand side of Eq. (34) with  $E = 0$ . We will use the following forms of the zero-energy Green functions:

$$G_0^{(2)}(\rho) = -\ln(\rho/R_e)/2\pi, \quad (37)$$

$$G_0^{(4)}(\rho) = 1/4\pi^2\rho^2, \quad (38)$$

$$G_0^{(6)}(\rho) = 1/4\pi^3\rho^4. \quad (39)$$

Equations (35) and (36) conserve angular momentum and parity. We will be interested in the case of positive parity (for  $D = 1$ ) and zero angular momentum (for  $D > 1$ ) so that  $f(\mathbf{x}) = f(x)$  and  $\phi(\mathbf{x}) = \phi(x)$ . Note also that if  $g_{12} = 0$ , the solution of Eqs. (35) and (36) is  $f(x) = 0$  and  $\phi(x) = \sqrt{2R_e^D}$ , indicating the absence of two-body and three-body interactions.

The quantity that we want to extract from solving Eqs. (35) and (36) is  $\tilde{f}(0) = \int_{\mathbf{x}} f(x)$ , which is proportional to the three-body scattering amplitude. Indeed, at large hyperradii  $\rho = \sqrt{x^2 + y^2}$  Eq. (34) gives  $\Psi \approx 1 + 3\tilde{f}(0)G_0^{(2D)}(\rho)$  or, explicitly,

$$\Psi = \begin{cases} 1 - 3\tilde{f}(0)\ln(\rho/R_e)/2\pi & \propto \ln(\rho/a_3), & D = 1, \\ 1 + 3\tilde{f}(0)/4\pi^2\rho^2 & \propto 1 - S_3/\rho^2, & D = 2, \\ 1 + 3\tilde{f}(0)/4\pi^3\rho^4 & \propto 1 - \Upsilon_3/\rho^4, & D = 3, \end{cases} \quad (40)$$

where we have introduced the three-body scattering length  $a_3$  in one dimension, surface  $S_3$  in two dimensions, and hypervolume  $\Upsilon_3$  in three dimensions:

$$a_3 = R_e \exp[2\pi/3\tilde{f}(0)], \quad D = 1, \quad (41)$$

$$S_3 = -3\tilde{f}(0)/4\pi^2, \quad D = 2, \quad (42)$$

$$\Upsilon_3 = -3\tilde{f}(0)/4\pi^3, \quad D = 3. \quad (43)$$

It is useful to note that for  $D = 2, 3$  the three-body potential  $g_3\delta(\sqrt{3}\mathbf{x}/2)\delta(\mathbf{y})$  with [42]

$$g_3 = -3(\sqrt{3}/2)^D \tilde{f}(0) \quad (44)$$

treated in the first Born approximation would produce the same scattered wave as Eqs. (40). Equations (42), (43), and (44) relate the three-body coupling constant  $g_3$  to the three-body scattering surface and hypervolume. The corresponding contribution to the energy density of a three-body-interacting condensate equals  $g_3 n^3/6$  in the weakly interacting regime, which is defined by  $|S_3|n \ll 1$  in two dimensions and by  $|\Upsilon_3|n^{4/3} \ll 1$  for  $D = 3$ . The quantity  $g_3/L^{2D}$  gives the energy shift for three (condensed) atoms in a large volume  $L^D$ . By solving the three-body problem nonperturbatively we

calculate the exact  $g_3$ , which can then be compared to the mean-field result given by Eq. (5).

The relation between  $a_3$  and the three-body energy shift in the case  $D = 1$  is slightly more subtle. Pastukhov [30] has recently shown that the ground-state energy density of a three-body-interacting one-dimensional Bose gas can be expanded in half-integer powers of the small parameter

$$g_3(n) = \sqrt{3}\pi/\ln(1/a_3n) \ll 1, \quad (45)$$

with the leading-order term equal to  $E/L = g_3(n)n^3/6$ . Although  $g_3$  given by Eq. (45) depends on  $n$ , one can replace  $1/n$  by another density-independent length scale  $l$ . If this scale is not exponentially different from  $1/n$ , the two small parameters are equivalent since they differ only by a higher-order term  $\sim g_3^2$ . By computing  $a_3$  we can thus compare Eqs. (5) and (45) which we expect to approach each other in the limit  $R_e/a_{12} \rightarrow 0$  (at fixed  $n$ ). Equivalently, one can say that in this limit Eq. (5) predicts the leading exponential dependence of the one-dimensional three-body scattering length

$$a_3 \propto \exp\left(\frac{\pi}{\sqrt{3}} \frac{\mu_{12}a_{12}}{R_e}\right) = \exp\left(\frac{2\pi}{3\sqrt{3}} \frac{a_{12}}{R_e}\right) \quad (46)$$

leaving, however, the preexponential factor unknown.

Returning to the task of determining  $\tilde{f}(0)$  from Eqs. (35) and (36) we note that the three-body problem in hand admits a zero-range description parametrized by  $a_{11}$ ,  $a_{12}$ , and  $R_e$  (see, however, Sec. IV C). Indeed, the sum  $\hat{L}f(x) + f(x)/g_{11}$  in Eq. (35) is well behaved in the limit  $r_0 \rightarrow 0$  since the singularity of  $\hat{L}f(x)$  gets canceled by the  $r_0$ -dependent term in  $1/g_{11}$  [see Eqs. (21) and (23)]. The parameter  $r_0$  thus drops out from Eq. (35),  $g_{11}$  being conveniently eliminated in favor of  $a_{11}$ . As far as Eq. (36) is concerned, one can just substitute the interaction term  $g_{12}\delta_{r_0}(\sqrt{3}x/2)$  by the Bethe-Peierls boundary conditions at  $x \rightarrow 0$ :

$$\phi(x) \propto |x| - 2a_{12}/\sqrt{3}, \quad D = 1, \quad (47)$$

$$\phi(x) \propto \ln(\sqrt{3}x/2a_{12}), \quad D = 2, \quad (48)$$

$$\phi(x) \propto 1 - 2a_{12}/\sqrt{3}x, \quad D = 3. \quad (49)$$

In other words, Eq. (36) is equivalent to

$$-\nabla_{\mathbf{x}}^2\phi(\mathbf{x}) = -\sqrt{2/R_e^D}f(\mathbf{x}), \quad (50)$$

supplemented by the boundary conditions (47)–(49).

From now on, for brevity, we choose to measure all distances in units of  $R_e$ . The function  $\tilde{f}(0)$  then depends on  $a_{11}$  and  $a_{12}$  (measured in units of  $R_e$ ) and its dimension is clear from Eq. (40).

The idea of solving Eqs. (35) and (47)–(50) is to eliminate  $\phi$  by inverting the Laplacian in Eq. (50) and then deal with a single integral equation for  $f$ . We perform this procedure in momentum space [the Fourier transform is defined by  $\tilde{F}(p) = \int_{\mathbf{x}} F(x)e^{-i\mathbf{p}\mathbf{x}}$ ] where Eq. (50) formally transforms into  $p^2\tilde{\phi}(p) = -\sqrt{2}\tilde{f}(p)$ . Note, however, that we can always add to  $\phi(\mathbf{x})$  a general solution of the Laplace equation  $-\nabla_{\mathbf{x}}^2\phi = 0$ , possibly singular at the origin. The solution of Eq. (50) in momentum space is thus  $-\sqrt{2}\tilde{f}(p)/p^2$  plus any linear combination of  $\delta(\mathbf{p})$  and  $1/p^2$ . The freedom of choosing the

corresponding coefficients is removed by Eq. (35) and the boundary conditions (47)–(49). The passage to momentum space in Eq. (35) is realized by rewriting the Fourier-space version of the operator

$$\begin{aligned} & (\hat{L} + 1/g_{11})\tilde{f}(p) \\ &= \left(\frac{2}{\sqrt{3}}\right)^{D-2} \sum_{\pm} \int \frac{\tilde{f}(q)}{p^2 \pm \mathbf{p}\mathbf{q} + q^2} \frac{d^D q}{(2\pi)^D} \\ &+ \tilde{f}(p) \begin{cases} 1/2|p| - a_{11}/2, & D = 1, \\ -(1/2\pi)\ln(pa_{11}e^\gamma/2), & D = 2, \\ -p/4\pi + 1/4\pi a_{11}, & D = 3. \end{cases} \end{aligned} \quad (51)$$

We now proceed to reformulating the boundary conditions (47)–(49) in momentum space. To this end let us first study the large- $x$  behavior of  $\phi(x)$  and  $f(x)$  and check that these functions indeed possess well-defined Fourier transforms. When two atoms are far away from the third one (large  $x$ ), the function  $\phi$  is approximately proportional to  $\Psi$  due to Eq. (12), which is equivalent to having small  $f$  in Eq. (32). Thus the large- $x$  asymptotic behavior of  $\phi(x)$  is given by Eq. (40) and, by calculating the second derivative of these asymptotes and using Eq. (50), we obtain the large- $x$  scaling  $f(x) \propto x^{-2D}$ . We conclude that the passage to momentum representation is straightforward for  $D > 1$ , where  $f(x)$  and  $\phi(x)$  are well behaved. By contrast, in one dimension  $\phi(x) \propto \ln|x|$  should be understood in the generalized sense by using a limit of a series of Fourier-transformable functions. In particular, we can use the relation  $K_0(\sqrt{\epsilon}|x|) \approx -\ln \frac{\sqrt{\epsilon}|x|e^\gamma}{2}$  valid for small  $\epsilon > 0$  and define a generalized Fourier transform of  $\ln|x|$  as

$$-\frac{\pi}{|p|} = \lim_{\epsilon \rightarrow +0} \left[ -\frac{\pi}{\sqrt{p^2 + \epsilon}} - 2\pi\delta(p) \ln \frac{\sqrt{\epsilon}e^\gamma}{2} \right]. \quad (52)$$

An immediate application of this formalism is the reformulation of the Bethe-Peierls boundary condition (47) in momentum space. Namely, for small  $x$  we have

$$\phi(x) = \int \tilde{\phi}(p) \frac{dp}{2\pi} - \frac{|x|}{2} \lim_{p \rightarrow \infty} p^2 \tilde{\phi}(p) + o(x), \quad (53)$$

where the integral is convergent, the singularity  $\tilde{\phi}(p) \propto 1/|p|$  being understood in the sense of Eq. (52). Comparing Eq. (53) with (47) and denoting  $C = \lim_{p \rightarrow \infty} p^2 \tilde{\phi}(p)$  gives us the Bethe-Peierls boundary condition in momentum space

$$\int \frac{\tilde{\phi}(p)}{C} \frac{dp}{2\pi} = \frac{a_{12}}{\sqrt{3}}. \quad (54)$$

Repeating the same procedure in two dimensions Eq. (48) transforms into

$$\int \left[ \frac{\tilde{\phi}(p)}{C} - \frac{1}{p^2 + \sigma} \right] \frac{d^2 p}{(2\pi)^2} = \frac{1}{2\pi} \ln \frac{a_{12}\sqrt{\sigma}e^\gamma}{\sqrt{3}}, \quad (55)$$

where  $\sigma$  is any positive number. In the case  $D = 3$ , Eq. (49) becomes

$$\int \left[ \frac{\tilde{\phi}(p)}{C} - \frac{1}{p^2} \right] \frac{d^3 p}{(2\pi)^3} = -\frac{\sqrt{3}}{8\pi a_{12}}. \quad (56)$$

The task of reformulating our problem in momentum space is thus over.

We now write the solution of Eq. (50) in the form

$$\tilde{\phi}(p) = \sqrt{2}(2\pi)^D \delta(\mathbf{p}) + \frac{C - \sqrt{2}\tilde{f}(p)}{p^2}. \quad (57)$$

Equation (57) is consistent with the definition of  $C$  (which is still unknown) and the coefficient in front of  $\delta(\mathbf{p})$  is dictated by Eq. (35) and by the fact that the operator (51) does not give rise to a delta function. We now eliminate  $\tilde{\phi}(p)$  by substituting Eq. (57) into Eqs. (35) and (54)–(56) and after simple manipulations we obtain the following results.

### A. One dimension

In one dimension we arrive at

$$\tilde{f}(0) = \frac{1}{a_{12}/\sqrt{3} + I^{(1)}(a_{11})}, \quad (58)$$

where the function  $I^{(1)}(a_{11}) = \int \frac{\chi(p)-1}{p^2} \frac{dp}{2\pi}$  is defined through the solution of

$$\begin{aligned} & \frac{\sqrt{3}}{2} \sum_{\pm} \int \frac{\chi(q)}{p^2 \pm pq + q^2} \frac{dq}{2\pi} \\ &+ \left( \frac{1}{2|p|} + \frac{1}{p^2} - \frac{a_{11}}{2} \right) \chi(p) = \frac{1}{p^2}, \end{aligned} \quad (59)$$

$C = \sqrt{2}\tilde{f}(0)$ , and  $\tilde{f}(p) = \tilde{f}(0)\chi(p)$ . Substituting Eq. (58) into Eq. (41)  $a_3$  factorizes into (we restore the dimensions here)

$$a_3 = R_e \exp\left(\frac{2\pi}{3\sqrt{3}} \frac{a_{12}}{R_e}\right) \exp\left[\frac{2\pi}{3} I^{(1)}\left(\frac{a_{11}}{R_e}\right)\right], \quad (60)$$

consistent with Eq. (46) in the limit of small  $R_e/a_{12}$ .

Let us now discuss the function  $I^{(1)}$ . For large  $a_{11}$  (weak atom-atom interaction) this function can be expanded in powers of  $\sqrt{-1/a_{11}}$ . In order to see this we rescale the momentum  $p = \sqrt{-1/a_{11}}z$  and rewrite Eq. (59) in the form

$$\begin{aligned} \chi(z) &= \frac{1}{1 + z^2/2} - \frac{1}{\sqrt{-a_{11}}} \frac{z^2}{1 + z^2/2} \\ &\times \left[ \frac{\sqrt{3}}{2} \sum_{\pm} \int \frac{\chi(y)}{z^2 \pm yz + y^2} \frac{dy}{2\pi} + \frac{\chi(z)}{2|z|} \right], \end{aligned} \quad (61)$$

which we then solve iteratively. In particular, the first iteration gives  $\chi(z) = 1/(1 + z^2/2)$  and provides the leading order term  $I^{(1)} \approx -\sqrt{-a_{11}}/8$ . The second iteration results in

$$I^{(1)} = -\sqrt{-\frac{a_{11}}{8}} + \frac{9 + 5\sqrt{3}\pi + 27 \ln(-a_{11}e^{-2\gamma}/2)}{36\pi} + o(1). \quad (62)$$

The solid and dashed lines in Fig. 1 show, respectively, the real and imaginary parts of  $I^{(1)}$  as a function of  $-1/a_{11}$  ( $= g_{11}/2$ ) obtained numerically. The dotted lines indicate the real and imaginary parts of the large- $a_{11}$  asymptote (62).

For negative  $a_{11}$  the solution is real and  $\text{Im}I^{(1)} \equiv 0$ . By contrast, for  $a_{11} > 0$  the function  $\chi(p)$  is characterized by simple poles at  $p = \pm(\kappa + i0)$ , where  $\kappa > 0$  is defined by Eq. (24) [this is also the point where the term in round brackets in Eq. (59) vanishes]. These poles correspond to the

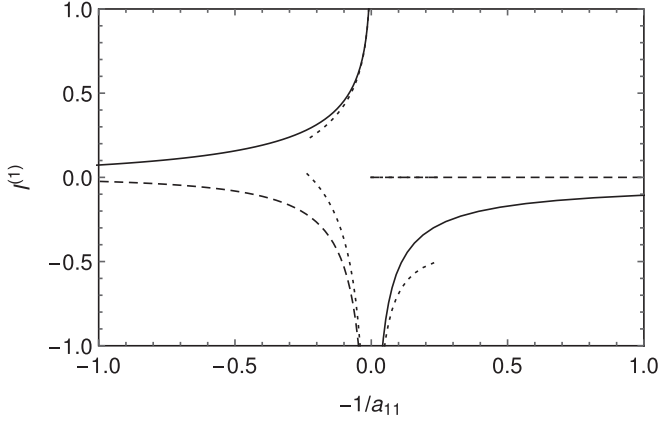


FIG. 1. Functions  $\text{Re}I^{(1)}$  (solid) and  $\text{Im}I^{(1)}$  (dashed) characterizing the dependence of the effective three-body interaction on  $a_{11}$  in one dimension [see Eqs. (58) and (40)].  $a_{11}$  is measured in units of  $R_g$ . The dotted curves correspond to the large- $a_{11}$  asymptote [Eq. (62)]. For  $a_{11} \rightarrow \pm 0$  one has  $I^{(1)} \approx -0.03$ .

three-body recombination to a dimer state, which, as found in Sec. III, exists only for positive  $a_{11}$ . One sees that  $I^{(1)}$  and, therefore,  $\tilde{f}(0)$  become complex reflecting the three-body loss. Technically, as one passes from positive to negative  $-1/a_{11}$ , the choice of the correct branch of the square root and logarithm in Eq. (62) is ensured by keeping  $-1/a_{11}$  just below the real axis.

### B. Two dimensions

The solution in the two-dimensional case can be written as

$$\tilde{f}(0) = \frac{2\pi}{\ln(a_{12}e^\gamma/\sqrt{3}) + 2\pi I^{(2)}(a_{11})}, \quad (63)$$

where  $I^{(2)}(a_{11}) = \int \frac{\chi(p)-1/(p^2+1)}{p^2} \frac{d^2p}{(2\pi)^2}$  and  $\chi$  satisfies

$$\sum_{\pm} \int \frac{\chi(q)}{p^2 \pm \mathbf{p}\mathbf{q} + q^2} \frac{d^2q}{(2\pi)^2} + \left( \frac{1}{p^2} - \frac{1}{2\pi} \ln \frac{a_{11}p e^\gamma}{2} \right) \chi(p) = \frac{1}{p^2}. \quad (64)$$

The three-body scattering surface is proportional to  $\tilde{f}(0)$  [see Eq. (42)] and the mean-field result (5) is recovered for weak attractive or repulsive atom-dimer interactions (small or large  $a_{12}$ ). As in the one-dimensional case we see that the dependence on  $a_{12}$  is analytic and for the complete solution of the problem one needs to know only  $I^{(2)}(a_{11})$ .

For a weak atom-atom background interaction (small or large  $a_{11}$ ), introducing the small parameter  $\lambda = 1/\ln(1/a_{11})$ , we can proceed iteratively in exactly the same manner as in the one-dimensional case. Namely, using the momentum rescaling  $p = \sqrt{\lambda}z$  one can see that to the leading order  $\chi(z) \approx 1/(1+z^2/2\pi)$  and after two iterations we have

$$I^{(2)} = \frac{\ln(2\pi\lambda)}{4\pi} + \lambda \frac{\ln(C\lambda)}{8\pi} + o(\lambda), \quad (65)$$

where  $C \approx 0.013$ .

In Fig. 2 we plot the real (solid) and imaginary (dashed) parts of  $I^{(2)}$  versus  $\lambda$  together with the asymptote (65) (dotted).

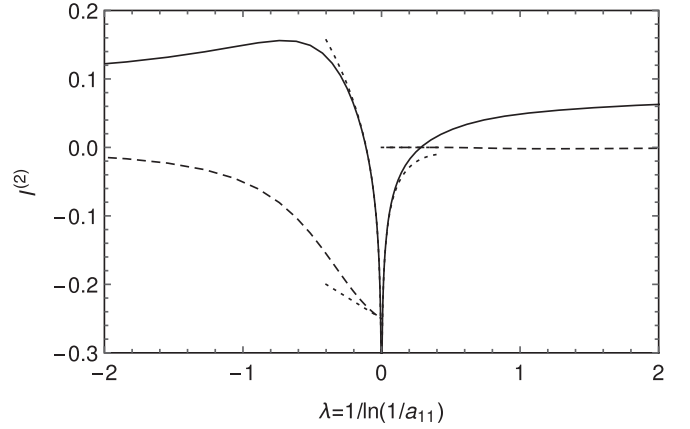


FIG. 2. Real and imaginary parts of  $I^{(2)}$  in the two-dimensional case. We use the same notations as in Fig. 1.

In the two-dimensional case  $\text{Im}I^{(2)}$  is always finite since there is always a dimer bound state available for the recombination (see Sec. III). However, for small positive  $\lambda$  the dimer is exponentially deep and small (its energy is proportional to  $1/a_{11}^2 = e^{-1/\lambda}$ ) so that the recombination in this limit is not captured by the power expansion Eq. (65).

Note that for small  $\lambda$  the characteristic momentum involved in the solution  $\chi(p)$  is  $\sqrt{\lambda}$ . Therefore, the asymptotic expansion (65) is also valid if, instead of the zero-range atom-atom interaction, we have a potential of a finite but sufficiently small range  $\ll 1/\sqrt{\lambda} = \sqrt{|\ln(1/a_{11})|}$ , characterized by the same scattering length  $a_{11}$ . In particular, one can have a purely repulsive potential which does not lead to a dimer state in our problem.

### C. Three dimensions

In three dimensions we have

$$\tilde{f}(0) = \frac{1}{-\sqrt{3}/8\pi a_{12} + I^{(3)}(a_{11})}, \quad (66)$$

where  $I^{(3)}(a_{11}) = \int \frac{\chi(p)}{p^2} \frac{d^3p}{(2\pi)^3}$  with  $\chi$  satisfying

$$\frac{2}{\sqrt{3}} \sum_{\pm} \int \frac{\chi(q)}{p^2 \pm \mathbf{p}\mathbf{q} + q^2} \frac{d^3q}{(2\pi)^3} + \left( \frac{1}{p^2} - \frac{p}{4\pi} + \frac{1}{4\pi a_{11}} \right) \chi(p) = \frac{1}{p^2}. \quad (67)$$

Here we also manage to separate the dependencies on the atom-dimer and atom-atom interactions. The mean-field solution (5) is retrieved for  $a_{12} \rightarrow 0$ . Calculating  $I^{(3)}$  is, however, more subtle than in the low-dimensional cases. Indeed, small hyperradii effectively correspond to high collision momenta and energies where the two-body scattering length is approximated by its background value  $a_{11}$ . Thus, at  $\rho \ll a_{11}$ , we deal with the Efimovian three-boson system which requires a three-body parameter or a cutoff momentum. Mathematically, this can be seen from Eq. (67) at momenta  $p \gg 1/a_{11}$ , where the dominant terms are the integral and  $-p\chi(p)/4\pi$ . The corresponding large-momentum behavior of  $\chi(p)$  is a linear combination of Efimov waves  $p^{\pm is_0-2}$  with  $s_0 \approx 1.00624$  [43].

The coefficients in this linear combination are fixed by introducing an external (three-body) parameter, phase, or momentum. Namely, one can set

$$\chi \propto \frac{\sin[s_0 \ln(p/p_0)]}{p^2} \quad (68)$$

as the asymptotic boundary condition for  $p \gg 1/a_{11}$ . Accordingly, the quantity  $I^{(3)}$  is, in fact, a function of  $a_{11}$  and the three-body parameter  $p_0$ . However, for small  $a_{11}$  the leading-order contribution to  $I^{(3)}$  is universal, i.e., independent of  $p_0$ . Indeed, for small  $a_{11}$  and momenta  $p \ll 1/|a_{11}|$  Eq. (67) reduces to  $(1/p^2 + 1/4\pi a_{11})\chi(p) = 1/p^2$ . The corresponding solution  $\chi = 1/(1 + p^2/4\pi a_{11})$  is characterized by the typical momentum  $\sqrt{a_{11}} \ll 1/a_{11}$  and leads to

$$I^{(3)} \approx \sqrt{a_{11}/4\pi}. \quad (69)$$

In order to estimate the next-order term we match  $\chi(p)$  with the Efimov wave (68) at momentum  $p \sim 1/|a_{11}|$  obtaining a contribution to  $I^{(3)}$  of the order of  $a_{11}^2$ .

It makes sense to study the case of larger  $a_{11}$  ( $\gtrsim R_e$ ) within our zero-range model, if we deal with a zero crossing near a narrow Feshbach resonance (large  $R_e$ ) which, in turn, lies in the vicinity of a broader Feshbach resonance (large  $a_{11}$ ). At the same time it is interesting to have a significant atom-dimer interaction (large  $a_{12}$ ) such that the two terms in the denominator of Eq. (66) are comparable. Then, in order to find the effective three-body force we also need to know the three-body and inelasticity parameters (or, equivalently, the real and imaginary parts of  $p_0$ ), which could be known from the Efimov loss spectroscopy near the broad resonance. Given the large number of parameters in this problem we just give a prescription for calculating  $I^{(3)}$ . Namely, one has to solve Eq. (67) with the boundary condition (68) at  $p \rightarrow \infty$  also requiring  $\chi \propto 1/(p - \kappa - i0)$  near the pole given by Eq. (26).

## V. DISCUSSION AND CONCLUSIONS

In this article we have expanded the idea that the bosonic model with a Feshbach-type atom-dimer conversion (1) near a two-body zero crossing can be reduced to a purely atomic model with an effective three-body interaction, which strongly depends on the atom-dimer conversion amplitude. As a particular example, we show that this mechanism of generating three-body forces can be used for stabilizing supersolid phases of two-dimensional dipoles.

Sections III and IV have been devoted to constructing a zero-range regularized version of the model (1) with a minimal set of parameters ( $a_{11}$ ,  $a_{12}$ , and  $R_e$ ). We have solved this model nonperturbatively in the two-body and three-body cases in all dimensions at the two-body zero crossing. Formulas (58), (63), and (66) give analytic dependencies of the three-body scattering amplitude on  $a_{12}$  in different dimensions. The dependence on  $a_{11}$  is found numerically and also analytically for weak atom-atom background interactions. In the three-dimensional case, our three-body zero-range model is Efimovian and requires an additional three-body parameter. We find, however, that for small  $|a_{11}|/R_e$ , effects associated with the Efimov physics are subleading.

These results show that for comparable and weak atom-dimer and atom-atom interactions (characterized by  $g_{12}$  and  $g_{11}$ , respectively), the three-body interaction is mostly influenced by  $g_{12}$ , consistent with the mean-field result (5). However, the convergence is not always uniform. For example, in the two-dimensional case, one can simultaneously decrease  $g_{12}$  and  $g_{11}$ , keeping both terms in the denominator of Eq. (63) comparable to (or even canceling) each other (resulting in a diverging three-body scattering surface). In the same spirit, we can use the nonperturbative three-dimensional formula Eq. (66) and predict a three-body resonance at  $\sqrt{3}R_e/8\pi a_{12} \approx \sqrt{a_{11}/4\pi R_e} \ll 1$ .

Inelastic three-body events manifest themselves through the appearance of an imaginary part of  $\tilde{f}(0)$ , which, in turn, comes from the complex  $I^{(D)}$  or complex atom-dimer scattering length  $a_{12}$ . The former reflects the three-body recombination to a dimer state and the latter the relaxation process in collisions of atoms with closed-channel dimers.

Several proposals on how to observe elastic three-body interactions experimentally are based on the following ideas. A repulsive three-body force could stabilize a system with attractive two-body interactions and make it self-trapped [16]. The structure and energies of few-body bound states, detectable spectroscopically, are also influenced by these forces [22,24–26]. Collective-mode frequency shifts in a trapped gas could be another experimentally observable signature of three-body interactions [32].

## ACKNOWLEDGMENTS

The research leading to these results received funding from the European Research Council (FP7/2007–2013 Grant Agreement No. 341197) and we acknowledge support from ANR Grant Droplets No. ANR-19-CE30-0003-02.

- [1] H. Kadau, M. Schmitt, M. Wenzel, C. Wink, T. Maier, I. Ferrier-Barbut, and T. Pfau, Observing the Rosensweig instability of a quantum ferrofluid, *Nature (London)* **530**, 194 (2016).
- [2] M. Schmitt, M. Wenzel, F. Böttcher, I. Ferrier-Barbut, and T. Pfau, Self-bound droplets of a dilute magnetic quantum liquid, *Nature (London)* **539**, 259 (2016).
- [3] I. Ferrier-Barbut, H. Kadau, M. Schmitt, M. Wenzel, and T. Pfau, Observation of Quantum Droplets in a Strongly Dipolar Bose Gas, *Phys. Rev. Lett.* **116**, 215301 (2016).

- [4] L. Chomaz, S. Baier, D. Petter, M. J. Mark, F. Wächtler, L. Santos, and F. Ferlaino, Quantum-Fluctuation-Driven Crossover from a Dilute Bose-Einstein Condensate to a Macrodroplet in a Dipolar Quantum Fluid, *Phys. Rev. X* **6**, 041039 (2016).
- [5] C. R. Cabrera, L. Tanzi, J. Sanz, B. Naylor, P. Thomas, P. Cheiney, and L. Tarruell, Quantum liquid droplets in a mixture of Bose-Einstein condensates, *Science* **359**, 301 (2017).



- [6] P. Cheiney, C. R. Cabrera, J. Sanz, B. Naylor, L. Tanzi, and L. Tarruell, Bright Soliton to Quantum Droplet Transition in a Mixture of Bose-Einstein Condensates, *Phys. Rev. Lett.* **120**, 135301 (2018).
- [7] G. Semeghini, G. Ferioli, L. Masi, C. Mazzinghi, L. Wolswijk, F. Minardi, M. Modugno, G. Modugno, M. Inguscio, and M. Fattori, Self-Bound Quantum Droplets of Atomic Mixtures in Free Space, *Phys. Rev. Lett.* **120**, 235301 (2018).
- [8] D. S. Petrov, Quantum Mechanical Stabilization of a Collapsing Bose-Bose Mixture, *Phys. Rev. Lett.* **115**, 155302 (2015).
- [9] F. Wächtler and L. Santos, Quantum filaments in dipolar Bose-Einstein condensates, *Phys. Rev. A* **93**, 061603(R) (2016).
- [10] R. N. Bisset, R. M. Wilson, D. Baillie, and P. B. Blakie, Ground-state phase diagram of a dipolar condensate with quantum fluctuations, *Phys. Rev. A* **94**, 033619 (2016).
- [11] L. Tanzi, E. Lucioni, F. Famà, J. Catani, A. Fioretti, C. Gabbanini, R. N. Bisset, L. Santos, and G. Modugno, Observation of a Dipolar Quantum Gas with Metastable Supersolid Properties, *Phys. Rev. Lett.* **122**, 130405 (2019).
- [12] L. Chomaz, D. Petter, P. Ilzhöfer, G. Natale, A. Trautmann, C. Politi, G. Durastante, R. M. W. van Bijnen, A. Patscheider, M. Sohmen, M. J. Mark, and F. Ferlaino, Long-Lived and Transient Supersolid Behaviors in Dipolar Quantum Gases, *Phys. Rev. X* **9**, 021012 (2019).
- [13] F. Böttcher, J.-N. Schmidt, M. Wenzel, J. Hertkorn, M. Guo, T. Langen, and T. Pfau, Transient Supersolid Properties in an Array of Dipolar Quantum Droplets, *Phys. Rev. X* **9**, 011051 (2019).
- [14] L. Tanzi, S. M. Rocuzzo, E. Lucioni, F. Famà, A. Fioretti, C. Gabbanini, G. Modugno, A. Recati, and S. Stringari, Supersolid symmetry breaking from compressional oscillations in a dipolar quantum gas, *Nature (London)* (2019), doi:10.1038/s41586-019-1568-6.
- [15] M. Guo, F. Böttcher, J. Hertkorn, J.-N. Schmidt, M. Wenzel, H. -P. Büchler, T. Langen, and T. Pfau, The low-energy Goldstone mode in a trapped dipolar supersolid, *Nature (London)* (2019), doi:10.1038/s41586-019-1569-5.
- [16] A. Bulgac, Dilute Quantum Droplets, *Phys. Rev. Lett.* **89**, 050402 (2002).
- [17] D. S. Petrov, Three-Body Interacting Bosons in Free Space, *Phys. Rev. Lett.* **112**, 103201 (2014).
- [18] K.-T. Xi and H. Saito, Droplet formation in a Bose-Einstein condensate with strong dipole-dipole interaction, *Phys. Rev. A* **93**, 011604(R) (2016).
- [19] R. N. Bisset and P. B. Blakie, Crystallization of a dilute atomic dipolar condensate, *Phys. Rev. A* **92**, 061603(R) (2015).
- [20] Z.-K. Lu, Y. Li, D. S. Petrov, and G. V. Shlyapnikov, Stable Dilute Supersolid of Two-Dimensional Dipolar Bosons, *Phys. Rev. Lett.* **115**, 075303 (2015).
- [21] A. Pricoupenko and D. S. Petrov, Dimer-dimer zero crossing and dilute dimerized liquid in a one-dimensional mixture, *Phys. Rev. A* **97**, 063616 (2018).
- [22] Y. Sekino and Y. Nishida, Quantum droplet of one-dimensional bosons with a three-body attraction, *Phys. Rev. A* **97**, 011602(R) (2018).
- [23] J. E. Drut, J. R. McKenney, W. S. Daza, C. L. Lin, and C. R. Ordóñez, Quantum Anomaly and Thermodynamics of One-Dimensional Fermions with Three-Body Interactions, *Phys. Rev. Lett.* **120**, 243002 (2018).
- [24] Y. Nishida, Universal bound states of one-dimensional bosons with two- and three-body attractions, *Phys. Rev. A* **97**, 061603(R) (2018).
- [25] L. Pricoupenko, Pure confinement-induced trimer in one-dimensional atomic waveguides, *Phys. Rev. A* **97**, 061604(R) (2018).
- [26] G. Guijarro, A. Pricoupenko, G. E. Astrakharchik, J. Boronat, and D. S. Petrov, One-dimensional three-boson problem with two- and three-body interactions, *Phys. Rev. A* **97**, 061605(R) (2018).
- [27] L. Pricoupenko, Three-body pseudopotential for atoms confined in one dimension, *Phys. Rev. A* **99**, 012711 (2019).
- [28] W. S. Daza, J. E. Drut, C. L. Lin, and C. R. Ordóñez, A quantum field-theoretical perspective on scale anomalies in 1D systems with three-body interactions, *Mod. Phys. Lett. A* **34**, 1950291 (2019).
- [29] J. R. McKenney and J. E. Drut, Fermi-Fermi crossover in the ground state of one-dimensional few-body systems with anomalous three-body interactions, *Phys. Rev. A* **99**, 013615 (2019).
- [30] V. Pastukhov, Ground-state properties of dilute one-dimensional Bose gas with three-body repulsion, *Phys. Lett. A* **383**, 894 (2019).
- [31] M. Valiente, Three-body repulsive forces among identical bosons in one dimension, *Phys. Rev. A* **100**, 013614 (2019).
- [32] M. Valiente and V. Pastukhov, Anomalous frequency shifts in a one-dimensional trapped Bose gas, *Phys. Rev. A* **99**, 053607 (2019).
- [33] L. Radzihovsky, P. B. Weichman, and J. I. Park, Superfluidity and phase transitions in a resonant Bose gas, *Ann. Phys. (NY)* **323**, 2376 (2008).
- [34] M. A. Baranov, A. Micheli, S. Ronen, and P. Zoller, Bilayer superfluidity of fermionic polar molecules: Many-body effects, *Phys. Rev. A* **83**, 043602 (2011).
- [35] Z. Shotan, O. Machtey, S. Kokkelmans, and L. Khaykovich, Three-Body Recombination at Vanishing Scattering Lengths in an Ultracold Bose Gas, *Phys. Rev. Lett.* **113**, 053202 (2014).
- [36] G. Quémener and J. L. Bohn, Electric field suppression of ultracold confined chemical reactions, *Phys. Rev. A* **81**, 060701(R) (2010).
- [37] A. Micheli, Z. Idziaszek, G. Pupillo, M. A. Baranov, P. Zoller, and P. S. Julienne, Universal Rates for Reactive Ultracold Polar Molecules in Reduced Dimensions, *Phys. Rev. Lett.* **105**, 073202 (2010).
- [38] A. Frisch, M. Mark, K. Aikawa, S. Baier, R. Grimm, A. Petrov, S. Kotochigova, G. Quémener, M. Lepers, O. Dulieu, and F. Ferlaino, Ultracold Dipolar Molecules Composed of Strongly Magnetic Atoms, *Phys. Rev. Lett.* **115**, 203201 (2015).
- [39] R. Stock, A. Silberfarb, E. L. Bolda, and I. H. Deutsch, Generalized Pseudopotentials for Higher Partial Wave Scattering, *Phys. Rev. Lett.* **94**, 023202 (2005).
- [40] K. Kanjilal and D. Blume, Coupled-channel pseudopotential description of the Feshbach resonance in two dimensions, *Phys. Rev. A* **73**, 060701(R) (2006).

- [41] D. S. Petrov, in *Proceedings of the Les Houches Summer Schools, Session 94*, edited by C. Salomon, G. V. Shlyapnikov, and L. F. Cugliandolo (Oxford University Press, Oxford, England, 2013).
- [42] The prefactor  $\sqrt{3}/2$  here [and also in Eqs. (36), (47)–(49)] comes from our definition of the Jacobi coordinates (28), according to which the atom-dimer distance equals  $\sqrt{3}x/2$ .
- [43] See, for example, p. 359 in E. Braaten and H.-W. Hammer, Universality in few-body systems with large scattering length, *Phys. Rep.* **428**, 259 (2006).